AD-A093 639 MARYLAND UNIV COLLEGE PARK DEPT OF PHYSICS AND ASTRONOMY F/G 20/9
COLLISIONAL DRIFT WAVES IN A PLASMA WITH ELECTRON TEMPERATURE I--ETC(U)
SEP 80 J F DRAKE, A B HASSAM DE-AC05-79ET-53044 NL
UNCLASSIFIED PHR-A1-058

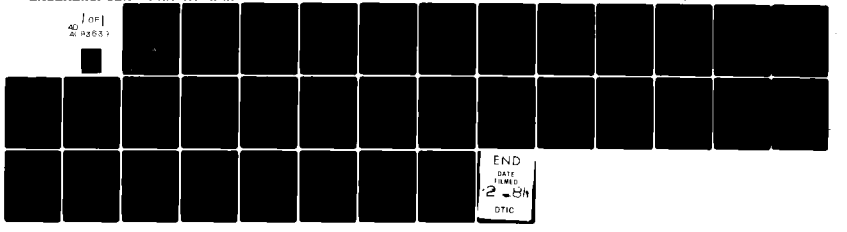

LEVEL II

Plasma Preprint PL #81-008

COLLISIONAL DRIFT WAVES IN A PLASMA WITH ELECTRON TEMPERATURE INHOMOGENEITY.

J. F. Drake and A. B. Hassam

Physics Publication Number 81-058

September 1, 1980

Contract DE-AC05-79ET-53044
Department of Energy

AD A093639

UNIVERSITY OF MARYLAND
DEPARTMENT OF PHYSICS AND ASTRONOMY
COLLEGE PARK, MARYLAND

Erratum

Column 6 in Table I should be

ν_{ei}(MHz)
.8
.6
1.4
1.0
1.3
.7

COLLISIONAL DRIFT WAVES IN A PLASMA WITH ELECTRON TEMPERATURE INHOMOGENEITY

J. F. Drake and A. B. Hassam
Department of Physics and Astronomy,
University of Maryland,
College Park, Maryland 20742

ABSTRACT

A fluid theory of collisional electrostatic drift waves in a plasma slab with magnetic shear is presented. Both electron temperature and density gradients are included. The equations are solved analytically in all relevant regions of the parameter space defined by the magnetic shear strength and the perpendicular wavelength and explicit expressions for the growth rates are given. For shear strengths appropriate for present-day tokamak discharges the temperature gradient produces potential wells which localize the mode in the electron resistive region, well inside the ion sound turning points. Mode stability arises from a competition between the destabilizing influence of the time dependent thermal force and the stabilizing influence of electron energy dissipation. Convective energy loss is not important for shear parameters of present-day fusion devices.

I. INTRODUCTION

Low frequency density fluctuations have been observed in a wide variety of magnetic confinement systems including tokamaks, stellarators, and multipoles.[1-7] Such fluctuations are important since they may enhance the crossfield particle or energy transport. The anomaly in the crossfield thermal transport coefficient has been most extensively documented in tokamak discharges although no causal relationship with the density fluctuations has been established.[8]

It is widely accepted that the observed density fluctuations arise from drift instabilities driven by the expansion-free energy associated with pressure gradients in confined plasmas. Extensive theoretical investigations of drift wave stability have been undertaken. In particular, the influence of magnetic shear on drift waves has been the subject of substantial controversy for nearly a decade. Pearlstein and Berk found that shear caused an outward convection of wave energy away from the mode rational surface ($\vec{k}\cdot\vec{B} = 0$) and they argued that drift wave stability resulted from a competition between this outward convection of energy and the release of expansion-free energy near the rational surface.[9] Later numerical and analytic calculations, while verifying the outgoing wave character of drift waves, demonstrated that pressure driven drift waves are always stable in a sheared magnetic field in slab geometry.[10]

The majority of investigations of drift wave stability have allowed gradients in the ambient density but not in the electron temperature. The dominant motivation for the study of drift waves, however, is the experimentally measured anomaly in the crossfield thermal conductivity of electrons in tokamak discharges; in these discharges, the temperature

gradient typically exceeds the density gradient. Thus, the inclusion of a temperature gradient in studies of drift wave stability is of critical importance. In fact, in recent numerical calculations, the temperature gradient was found to alter the entire structure of the mode.[11,12] It was found that the drift wave no longer had the character of an outward propagating wave but remained localized in the vicinity of the mode rational surface, well within the "ion sound turning points."[9] The outward convection of the wave energy therefore does not have a stabilizing influence on the mode if a temperature gradient is present. This localization by the temperature gradient appears both in the presence or absence of electron-ion collisions, ν_e. In the collisionless limit[11] the mode remains stable even when the convective energy loss can be neglected because of Landau absorption of wave energy by electrons in the vicinity of the rational surface. In the collisional limit, $\omega < \nu_e$, on the other hand, the wave can be destabilized by the temperature gradient if the velocity dependence of electron-ion collisions is taken into account.[12]

In the present paper we investigate the structure of collisional drift waves in a sheared magnetic field with both density and temperature gradients. We employ a fluid treatment which complements the kinetic treatment of Ref. 12 but which allows us to solve for the frequencies and growth or damping rates of the mode analytically. Our conclusions are in qualitative agreement with the conclusions of Ref. 12. The temperature gradient acts both to localize and to destabilize the drift wave. For parameters typical of present-day tokamaks, we find the modes to be strongly localized in the vicinity of the mode rational surface, well inside the ion sound surface. As the shear is increased, the modes become less and less localized and, eventually, for very strong shear the asymptotic

behavior of the mode far from the rational surface assumes the outgoing-wave structure of Pearlstein and Berk.

The relative stability of the mode results from a competition between the destabilizing influence of the "time dependent thermal force"[13] and local resistive energy absorption by the electrons. Thus, the mechanism for destabilization of the drift mode is the same as that of the temperature gradient driven microtearing mode.[14] For parameters appropriate for current tokamak discharges (in which there are still typically many modes with $\omega < \nu_e$) these drift modes may be unstable. We have, however, not included finite β corrections which were found to be stabilizing in Ref. 12.

The effect of temperature gradients on collisional drift waves was also studied by Chen et al.[15] Their analysis was based on Braginskii's fluid equations,[16] but they only solved the equations in the strong shear limit. Consistent with our strong shear results, they found that the temperature gradient does not localize the drift mode. However, their solutions differ from ours in this limit in that ∇T_e had no destabilizing influence on the mode. The time dependent thermal force, which is the source of instability, is a higher order correction to the thermal force and is not included in the equations of Braginskii;[13] hence, this force did not appear in their equations.

The fluid theory presented in this paper employs the Braginskii transport equations modified as described in Ref. 13. The derivation of the basic equations describing the linear drift mode are presented in Section II. In Section III the structure of the drift wave is examined as a function of magnetic shear, as represented by the dimensionless parameter $S = (M/m)(L_T/L_s)^2(\omega_{*T}/\nu_e)$, and perpendicular wavelength, $k\rho_s$, where M and m

are the ion and electron mass, L_s and L_T are the shear and temperature scale lengths, k is the perpendicular wavenumber, ρ_s is the ion Larmor radius based on T_e, and $\omega_{*T} = k\rho_s v_s/L_T$ is the diamagnetic frequency. The structure of the mode falls into four basic categories in this shear-wavelength parameter space (see Fig. 1). Eigenfunctions and eigenvalues of the drift wave are calculated analytically in each of these categories. A summary of our results appears in Section IV where we also discuss the relevance of the results to present magnetic fusion confinement schemes.

II. EQUATIONS

We consider a plasma slab with inhomogeneous temperature $T_e(x)$ and density $n(x)$, with the inhomogeneity scale lengths being L_n and L_T, respectively. The plasma slab is immersed in a sheared magnetic field $\vec{B} = B_o(\hat{z} + y\hat{x}/L_s)$. We take the ions to be cold and assume that magnetic fluctuations can be neglected (a low β assumption). As mentioned in the introduction, we employ Braginskii's fluid equations,[16] supplemented by the higher order corrections obtained in Ref. 13, to describe the plasma dynamics. For electric potential fluctuations $\tilde{\phi}(\vec{x},t) = \tilde{\phi}(x)\exp[i(ky-\omega t)]$, the linearized fluid equations are:

$$\omega\tilde{n} = \omega_{*n}\tilde{\phi} - k_\parallel(\tilde{j}_\parallel/ne) + k_\parallel\tilde{v}_{\parallel i} , \tag{1a}$$

$$\eta\,\tilde{j}_\parallel = -i(T/e)\,k_\parallel\,(\tilde{\phi} - \tilde{n} - \hat{\sigma}\,\tilde{T}) , \tag{1b}$$

$$[\omega + (2/3)i\,k_\parallel^2\,(\kappa_\parallel/n)]\,\tilde{T} = \omega_{*T}\tilde{\phi} - (2/3)(1+\alpha)\,k_\parallel\,[(\tilde{j}_\parallel/ne) - \tilde{v}_{\parallel i}] , \tag{1c}$$

$$\omega\rho_s^2\,\nabla^2\tilde{\phi} = -\,k_\parallel(\tilde{j}_\parallel/ne) , \tag{1d}$$

$$\omega\,M\,\tilde{v}_{\parallel i} = T\,k_\parallel\,(\tilde{n} + \tilde{T}) , \tag{1e}$$

where

$$\hat{\sigma} \equiv 1 + \alpha + i\,\alpha\alpha'(\omega/\nu_e) , \qquad \nu_e \equiv (4/3)(2\pi)^{1/2}\ell n\,\Lambda\,(ne^4/m^{1/2}T_e^{3/2}) ,$$

$$\eta \equiv .51\,m\,\nu_e/ne^2, \qquad \rho_s^2 \equiv M\,T/e^2B^2,$$

$$\kappa_{\parallel} \equiv 1.61\ T/\eta e^2 , \qquad \alpha = .71 ,$$

and tildes denote perturbed quantities. The perturbations $\tilde{n}$, $\tilde{T}$, and $\tilde{\phi}$ are normalized to n, T, and T/e, respectively, and the operator $\nabla^2 \to \partial^2/\partial x^2 - k^2$. The quantity α' is a numerical coefficient that appears as factor multiplying the time dependent thermal force.[13] An accurate and reliable value of α' has not yet been computed; for a Lorentz collision model,[17] the value of α' is 105/16, while a variational calculation[18] including electron-electron collisions with $Z = n_e/n_i = 1$ yielded the value .54. Since the time dependent thermal force is the mechanism responsible for destabilizing the present mode and because of the wide disparity in the values of α' just quoted, we have left the value of α' unspecified.

Equations (1)-(5) represent, respectively, the equation of continuity, parallel force balance for electrons with the term proportional to ω/ν_e being the time dependent thermal force, parallel electron heat flow, the parallel component of the curl of the one fluid momentum equation, and the parallel one fluid force balance equation. We have defined the parallel wavenumber $k_{\parallel} \equiv kx/L_s$.

It will be shown later that except for the case of very strong shear, ($S >> L_s/L_n$), $\tilde{v}_{\parallel i}$ can be neglected in Eqs. (1a) and (1c) in a self-consistent manner. This approximation is equivalent to discarding the "sound term" of the Pearlstein-Berk equation. Equations (1a)-(1d) can then be reduced to the eigenvalue equation

$$\partial^2\hat{\phi}/\partial s^2 + iV\hat{\phi} = 0 , \qquad (2)$$

where

$$\hat{S}V \equiv b + \frac{\delta s^2(1+\kappa s^2)}{D(s)} - \frac{\hat{\sigma}(\omega_{*T}/\omega)s^2}{D(s)} ,$$

$$\delta \equiv 1 - \omega_{*n}/\omega , \qquad \kappa = 1.07 ,$$

$$D(s) \equiv 1 + (1+\kappa+\gamma)s^2 + \kappa s^4 ,$$

$$\hat{S} \equiv (\omega_{*T}/\omega)S , \qquad b \equiv k_\theta^2 \rho_s^2 ,$$

$$\gamma \equiv (2/3)(1+\alpha)\hat{\sigma} ,$$

and where $s = [\exp(i\pi/4)](x/\Delta_D)$, with Δ_D defined by $k_\parallel'^2 \Delta_D^2 D_\parallel = \omega$, and $D_\parallel = T/(.51m\nu_e)$ is the parallel electron diffusion coefficient. The independent parameter s lies approximately along the line $\exp(-i\pi/4)$ with respect to the real x axis. We will solve the eigenvalue equation along this rotated axis and verify that the asymptotic solution corresponds to either a bounded or outgoing wave along the real x axis.

Although the expression for the potential V in Eq. (2) appears somewhat complicated, its general structural dependence on s can be readily discerned. In fact, for practical purposes, the true potential can be replaced by the model potential V_m given by

$$V_m \propto b + \frac{\delta s^2}{1+s^2} - \frac{\hat{\sigma}(\omega_{*T}/\omega)}{(1+s^2)^2} s^2 . \qquad (3)$$

The actual potential given in Eq. (2) reduces to this model in the limit $\kappa = 1$, $\gamma = 0$. In the absence of ω_{*T}, this model potential has two turning points (nearly on the real s axis for $\delta < 0$), one on either side of the

rational surface (s = 0). No solution localized between these turning points exists, however, because the potential is evanescent between the turning points ($V^2\tilde{\phi} = 0$ along the real axis). The only possible solution for $\omega_{*T} = 0$ is a solution which is bounded between this inner turning point and the outer sound turning point. In the presence of a temperature gradient, however, the foregoing potential has four turning points, two on either side of the rational surface. A localized solution between each of these turning points is now possible if δ has the appropriate sign.

Our general procedure in solving Eq. (2) is to assume that $L_T/L_n \sim O(1)$, and to examine the structure of the potential V as a function of the parameters S and b. [In most magnetized plasma of interest, L_T and L_n are comparable and, in keeping this ratio fixed, we greatly reduce the parameter space and hence the number of possible parametric regions.] When the shear S is very weak, we find that the two turning points on either side of the rational surface are nearly coincident (Region I of Fig. 1). The potential well then becomes approximately parabolic near the turning points and bounded solutions of the resulting Weber equation can be obtained. These solutions correspond to the bounded solutions obtained analytically in Ref. 12.

As we move from Region I to Region II of Fig. 1, the two turning points begin to separate and the inner turning point moves toward s=0. In this region, the solution of the Airy equation near the outer turning point is matched to the solution of a parabolic cylinder equation in the vicinity of s = 0. In Region III, the shear S is large; in this case, the potential is shallow and a "constant $\tilde{\phi}$ approximation" can be made to solve the equation. This constant $\tilde{\phi}$ solution near s ≃ 1 is matched to an evanescent solution for s >> 1 which is again localized well within the ion sound

turning point. Finally, in the case of very strong shear in Region IV of Fig. 1, the "constant $\tilde{\phi}$" solution for $s \sim 1$ is joined to the Pearlstein-Berk outgoing wave solution. In this region, our solution is consistent with the solutions obtained by Chen et al.[15] for drift waves with a temperature gradient.

The detailed solutions of Eq. (2) are described in the next section.

III. ANALYTIC SOLUTIONS

As previously discussed, Eq. (2) can be solved in the four regions of parameter space defined by S and b as shown in Fig. 2. We now examine each of the regions in detail.

A. Region I: $S \ll b^{3/2}, 1$

When the shear is very weak (i.e., as $S \to 0$) the mode will tend to localize itself in a region where the right-hand side of Eq. (2) is small so that $V(s) \propto S^{-1}$ remains finite. The existence of such a localized mode requires a second order turning point ($\partial V/\partial s = 0$) . In the limit $S \to 0$, we therefore obtain the dispersion relation by requiring that the two turning points, given by solution of the biquadratic equation,

$$\kappa(b+\delta)s_t^4 + [(1+\kappa+\gamma)b + \delta - \hat{\sigma}(\omega_{*T}/\omega)]s_t^2 + b = 0 \ , \tag{4a}$$

merge, or

$$[(1+\kappa+\gamma)b + \delta - \hat{\sigma}(\omega_{*T}/\omega)]^2 = 4\kappa b(b+\delta) \ . \tag{4b}$$

The lowest order dispersion relation obtained from (4b) is

$$\omega_o = [\omega_{*n} + 1.71\ \omega_{*T}](1 - 2.07\ c_1 b^{1/2} + .71 i\alpha' \omega_{*T}/\nu_e) \qquad b \ll 1 \ ,$$

$$\omega_o = .28\ \frac{\omega_{*T}}{b}\left(1 + .08 i\alpha' \frac{\omega_{*T}}{b\nu_e}\right) \qquad b \gg 1, \quad \eta_e \gg 1,$$

$$c_1 \equiv \left(\frac{1.71\ \eta_e}{1 + 1.71\ \eta_e}\right)^{1/2} \ , \tag{5}$$

where the root for $b \gg 1$ has only been given for $\eta_e \gg 1$ for simplicity of expression. The location of the double root is given by

$$s_o^2 = b^{1/2}/c_1 , \qquad b \ll 1 ,$$

$$s_o^2 = (1/\kappa)^{1/2} = 0.97 \qquad b \gg 1 , \quad \eta_e \gg 1 . \tag{6}$$

Note that the existence of a double root requires that η_e be nonzero ($\eta_e > 1$ for $b \gg 1$). In the absence of shear, there are no stabilizing terms in the expression for ω in Eq. (5) and so the time dependent thermal force destabilizes the mode.

When S is finite, the roots will split from the expression given in Eq. (6) by an amount Δs corresponding to a shift $\Delta\omega = \omega - \omega_o$ in the eigenvalue. By expanding V(s) around S_o, we obtain the eigenvalue equation

$$\partial^2\hat{\phi}/\partial s^2 + \left[\frac{4ib}{\hat{S}\, s_o^2\, D(s_o)}\right]\left[(s-s_o)^2-(\Delta s)^2\right]\hat{\phi} = 0 , \tag{7}$$

where

$$\Delta s \equiv \frac{\left\{\left[(1+\kappa+\gamma)b + \delta - \hat{\sigma}(\omega_{*T}/\omega)\right]^2 - 4\kappa b(b+\delta)\right\}^{1/2}}{4\kappa s_o(b+\delta)} . \tag{8}$$

The bounded solutions to this equation yield expressions for the shift in the eigenvalue ω_1,

$$(\omega_1/\omega_0) = -1.6\, c_1^{5/2} \exp(i\pi/4)(S/b^{1/2})^{1/2} \qquad b \ll 1 ,$$

$$(\omega_1/\omega_0) = -1.6 \exp(i\pi/4) S^{1/2} \qquad b \gg 1 , \quad \eta_e \gg 1 , \tag{9}$$

where, again, for simplicity, we have assumed $n_e \gg 1$. Since Im $\omega_1 < 0$, shear has a stabilizing influence on the drift wave even though the mode is bounded. This damping arises from electron resisitive dissipation and from parallel heat conduction. The instability drives a temperature perturbation $\hat{T}_e$ [see Eq. (1c)] which is dissipated by parallel diffusion along $\vec{B}$ and is therefore stabilizing. The overall stability of the mode results from the stabilizing influence of this local dissipation and the destabilizing influence of the time dependent thermal force.

The localization of the mode is of extent Δs around s_o. The parabolic expansion of the potential well around s_o therefore requires $\Delta s \ll s_o$ or

$$S \ll b^{3/2}, \qquad b \ll 1,$$

$$S \ll 1, \qquad b \gg 1. \tag{10}$$

We must also check, of course, that the solution obtained from Eq. (7) is bounded along the real x axis. In Fig. 2 we show the anti-Stokes (solid) and Stokes (dashed) lines for the potential V with eigenvalues given in Eqs. (5) and (7). The dashed lines are constant phase lines of the eikonal $\exp\{i \int^s ds' \, [i\, V(s')]^{1/2}\}$ while the solid lines are the constant amplitude lines of this eikonal. The solution which is evanescent along the Stokes line emanating from the turning point s_2 in Fig. 2 is evanescent throughout region B to the right of the anti-Stokes lines in this figure. Since region B includes the real x axis, our solution is also bounded along this axis.

For the eigenvalues given in Eq. (5), the sound turning point lies on the real axis at $|x| \propto x_s(1+b)^{1/2}$ with $x_s = \omega/k_\parallel' c_s$, which is well outside

of the region $x \sim \Delta_D$ where this mode is localized. The neglect of the parallel ion dynamics is therefore well justified.

B. Region II: $b^{3/2} < S < 1$

In the weak shear limit previously discussed, the mode was localized near $s_o \sim b^{1/4}$ (for $b \ll 1$), the two turning points being separated by a distance $\Delta s \sim (S/b^{1/2})^{1/4} \ll s_o$. As the shear is increased, the turning points separate until $S \sim b^{3/2}$, $\Delta s \sim s_o$. At this point the inner turning point s_1 is near the origin while the outer turning point is around $s_2 \sim b^{1/4} \sim S^{1/6} \ll 1$. In Region II of Fig. 1, we therefore look for a solution with $s_1 \ll s_2 \ll 1$.

When $b \ll 1$, the positions of the turning points s_1 and s_2 can be calculated as

$$s_2^2 = [\hat{\sigma}(\omega_{*T}/\omega) - \delta]/\delta\kappa \ ,$$

$$s_1^2 = b/(\delta\kappa\, s_2^2) \ . \tag{11}$$

Defining a new variable $p \equiv s/s_2$ and assuming $s \ll 1$, we can rewrite Eq. (2)

$$\partial^2\hat{\phi}/\partial p^2 - Q(p^2-\epsilon^2)(p^2-1)\hat{\phi} = 0 \ , \tag{12}$$

where

$$\epsilon^2 \equiv s_1^2/s_2^2 \ll 1 \ ,$$

$$Q \equiv -i\,\delta\kappa\, s_2^6/S \ . \tag{13}$$

We solve this equation by assuming that Q is a large parameter, and matching the Airy solution of Eq. (12) near p = 1 with the solution of the parabolic cylinder equation in the region $p^2 \approx \varepsilon^2 \approx 0$ through a WKB region $\varepsilon < p < 1$. The solution for $\tilde{\phi}$ near p = 1 which is decaying for p > 1 is given by $\tilde{\phi} = \mathrm{Ai}[(2Q)^{1/3}(p-1)]$. [19] The WKB solution which matches the p<1 behavior of this function is given by

$$\tilde{\phi} \sim \sin\ [Q^{1/2}(1-p^2)^{3/2}/3 + \pi/4] \ . \tag{14}$$

Near the origin this solution breaks down but Eq. (12) simplifies to

$$\partial^2\tilde{\phi}/\partial p^2 + Q(p^2-\varepsilon^2)\tilde{\phi} = 0 \ , \tag{15}$$

which is the parabolic cylinder equation.[9] We are actually only interested in solutions for which $\varepsilon^2 Q^{1/2} \ll 1$, i.e., the inner turning point can be entirely neglected. That $\varepsilon^2 Q^{1/2}$ is actually small shall be demonstrated <u>a posteriori</u>. Equation (15) now becomes a Bessel equation with the solution[19]

$$\tilde{\phi} = p^{1/2}\ C_{1/4}\ [Q^{1/2}p^2/2] \ , \tag{16}$$

where C_ν is Y_ν for $\tilde{\phi}$ even and J_ν for $\tilde{\phi}$ odd. The dispersion relation is then easily obtained by matching the asymptotic solution for $\tilde{\phi}$ in Eq. (16) with the small argument limit of $\tilde{\phi}$ in Eq. (14). We find

$$Q^{1/2} = (n + 1/4)3\pi/2 \ , \tag{17}$$

where n is a positive integer. For $n > 0$, the solution of this dispersion relation yields a Stokes structure which is similar to that shown in Fig. 2 except that the inner turning points are close to the origin. For $n < 0$, the Stokes structure is entirely different and our evanescent solution for $p \gg 1$ does not correpond to an evanescent solution along the real axis. The dispersion relation in Eq. (17) can be solved for the eigenvalue, viz.,

$$\omega = \omega_{*n} + 1.71\omega_{*T} + (1.2i/c_1^2)\alpha'(\omega_{*T}^2/\nu_e) - c_2 \exp(i\pi/6)\, S^{1/3}\omega_{*T}$$

$$c_2 = 2.81\,(1 + 1.71\eta_e)\,(n + 1/4)^{2/3}\, c_1^{4/3} \,. \qquad (18)$$

In the absence of the destabilizing influence of the time dependent thermal force, the mode is damped at a rate which scales as $S^{1/3}$. The location of the turning points can be calculated with the expression for ω given in Eq. (18). We find $s_2 \sim S^{1/6}$, while $s_1 \sim b^{1/2}/S^{1/6}$. The condition $s_1 \ll s_2$ then requires

$$S \gg b^{3/2} \,, \qquad (19)$$

which also guarantees that $\varepsilon^2 Q^{1/2} \ll 1$. The assumption $s_2 \ll 1$ along with the requirement $\mathrm{Im}\omega \ll \mathrm{Re}\omega$ requires

$$S \ll 1 \,. \qquad (20)$$

Region III: $1 < S \ll L_s/L_T$

When S is very large, the potential $V \sim S^{-1}$ is weak and the drift wave is no longer localized in the region $s \sim 1$, i.e., the shear prevents strong localization of the mode. However, in Region III we can still obtain solutions which are localized within the ion sound turning point. Equation (2) is solved in the two regions $s \ll S$ and $s \gg S^{1/2}$ and the solutions are matched in the overlap region $S^{1/2} < s < S$. When $s \ll S$, Eq. (2) can be approximated as

$$\partial^2\tilde{\phi}/\partial s^2 - \frac{i}{\hat{S}\, D(s)} \left\{ [1+(\kappa+\gamma)s^2]\delta + \hat{\sigma}(\omega_{*T}/\omega)s^2 \right\} \tilde{\phi} = 0 \ , \qquad (21)$$

where we have neglected $(b+\delta)/S \sim S^{-2}$ (to be checked self-consistently). Since S is large, this equation can be solved iteratively. To lowest order, $\tilde{\phi} \simeq$ const. Corrections are obtained by integrating Eq. (21),

$$\tilde{\phi}(s)/\tilde{\phi}(o) \simeq 1 + \frac{i}{\hat{S}} \int_o^s ds' \int_o^{s'} \frac{ds''}{D(s'')} \left\{ [1+(\kappa+\gamma)s''^2]\delta + \hat{\sigma}(\omega_{*T}/\omega)\ s''^2 \right\}$$

$$\simeq 1 + i(s/\hat{S}) [\delta I_1 + \hat{\sigma}(\omega_{*T}/\omega) I_2] \ , \qquad (22)$$

where

$$I_1 \equiv \int_o^\infty ds\ [1+(\kappa+\gamma)s^2]/D(s) = 5.0 \ ,$$

$$I_2 \equiv \int_o^\infty ds\ s^2/D(s) = 1.2 \ ,$$

and the second step in (22) is valid for $1 \ll s \ll S$. In the region $S^{1/2} \ll s$, Eq. (21) simplifies to

$$\partial^2\hat{\phi}/\partial s^2 + i[(b+\delta)/\hat{S}]\hat{\phi} = 0 \ , \tag{23}$$

with the bounded solution

$$\hat{\phi}(s) \sim \exp\left\{[(b+\delta)/\hat{S}]^{1/2} \exp(3\pi i/4)\right\} \ . \tag{24}$$

Matching the two solutions in Eqs. (22) and (24), we find the dispersion relation

$$(b+\delta)^{1/2} = e^{-i\pi/4}\, \hat{S}^{-1/2}\, [\delta I_1 + \hat{\sigma}(\omega_{*T}/\omega) I_2] \tag{25}$$

and the corresponding eigenvalue

$$\omega = \frac{\omega_{*n}}{1+b}(1 - i\, c_3/S) \ ,$$

$$c_3 \equiv (4.4/\eta_e)\left(\eta_e - 2.4\,\frac{b}{1+b}\right)^2 \ , \tag{26}$$

which has a real frequency which is characteristic of the drift wave without η_e. Note also that this mode is always stable. In addition to the requirement

$$S \gg 1 \ , \tag{27}$$

which was invoked to justify the iteration procedure, we require $\mathrm{Re}(b+\delta)^{1/2} > 0$ so that $\hat{\phi}$ in Eq. (24) is bounded. With the solution given in Eqs. (25) and (26), this requires $\eta_e \gtrsim b/(1+b)$ so that this solution is only possible when η_e is nonzero. Finally, we require that the mode be localized with the ion sound turning point. The scale length of the mode

is $\rho_s/(b+\delta)^{1/2}$, while the ion sound turning point is given by $x_s(b+\delta)^{1/2}$; so our solution is valid when

$$S << x_s/\rho_s \sim L_s/L_n \ . \tag{28}$$

When this inequality is violated, we must include the ion sound term in the outer solution.

Region IV: $S > L_s/L_n$

In this strong shear limit the ion sound term is retained and the equation for $\tilde{\phi}$ in the outer region is

$$\left[\frac{\partial^2}{\partial s^2} + i\,\frac{b+\delta}{\hat{S}} - \frac{\Delta_D^4}{x_s^2\rho_s^2}\,s^2\right]\hat{\phi} = 0 \ . \tag{29}$$

The solution of this parabolic cylinder equation with the outgoing wave boundary condition along the real x axis is

$$\hat{\phi} = U(a,p) = D_{-a-1/2}(p) \tag{30}$$

where

$$p^2 = 2\,s^2\,\Delta_D^2/x_s\rho_s \ ,$$

$$a = (b+\delta)x_s/2i\rho_s \ , \tag{31}$$

and $D_a(p)$ is Whittaker's function.[19] The logarithmic derivative of this solution as $s \to 0$ is

$$\frac{1}{\hat{\phi}}\frac{\partial\hat{\phi}}{\partial s}\bigg|_{s=0} \simeq -2\left(\frac{\Delta_D^2}{x_s\rho_s}\right)^{1/2}\frac{\Gamma(\frac{3}{4}+\frac{a}{2})}{\Gamma(\frac{1}{4}+\frac{a}{2})} . \tag{32}$$

Equating this expression to the logarithmic derivative of the solution for the inner region given in Eq. (23), we obtain the dispersion relation

$$\frac{\Gamma(\frac{3}{4}+\frac{a}{2})}{\Gamma(\frac{1}{4}+\frac{a}{2})} = \frac{-i}{2}\left(\frac{x_s}{\rho_s\hat{S}}\right)^{1/2}\left[\delta I_1 + \sigma(\hat{\omega}_{*T}/\omega) I_2\right] . \tag{33}$$

When $S \ll (L_s/L_n)$, the solution to this dispersion relation corresponds to $a \gg 1$ and simply reduces to Eq. (26). The ion sound term is not important in this limit. When this inequality is reversed (Region IV of Fig. 1), $\Gamma(1/4 + a/2) \sim (S\, L_n/L_s)^{1/2} \gg 1$ and the solution is given by $a \simeq -1/2$ or

$$\omega = \frac{\omega_{*n}}{1+b}\left[1 - i\frac{L_n}{L_s} + \left(\frac{4c_2}{\pi}\right)^{1/2}\left(\frac{L_n}{S\,L_s}\right)^{1/2}\right] . \tag{34}$$

The damping term in Eq. (34) corresponds to the usual convective energy loss in a sheared magnetic field. The temperature gradient, on the other hand, simply causes a shift in the real frequency of the mode in this strong shear regime. The destabilizing influence of the time dependent thermal force, though present, is small in this limit. The dispersion relation in Eq. (34) corresponds to that given in Ref. 15.

III. SUMMARY AND DISCUSSION

The collisional drift wave in the presence of ∇T_e falls into four distinct regimes as a function of magnetic shear and the perpendicular wavelength. These four regions are shown in the S-b phase space in Fig. 1, where $S = (M/m)(L_T^2/L_s^2)\omega_{*T}/\nu_e$ is the dimensionless shear and $b = k_\perp^2\rho_s^2$ is the perpendicular wavelength. In Region I, the shear is weak and the modes are strongly localized on either side of the rational surface at $x \sim \pm \Delta_D = \pm(\omega/k_\parallel'^2 D_\parallel)^{1/2}$. In Region II, the shear is somewhat stronger and the mode penetrates to the rational surface but is still localized inside the distance $|x| < \Delta_D$. In Region III, the shear is strong enough to prevent strong localization of the mode within the distance $|x| < \Delta_D$, but is sufficiently weak that the mode is still localized well within the ion sound turning points [$|x| \lesssim \rho_s(L_s/L_n)(1+b)^{-1/2}$]. Finally, when the shear is very strong, the mode assumes the usual outward propagating structure characteristic of the drift wave with $\nabla T_e = 0$. In Regions I and II, the real frequency of the mode scales roughly as $(\omega_{*T} + \omega_{*n})/(1+b)$ and is determined by the electron dynamics in the region $x \sim \Delta_D$. In Regions III and IV, the frequency is $\omega \simeq \omega_{*n}/(1+b)$ and is given by the plasma dynamics ouside the electron dissipative region $|x| \gg \Delta_D$.

The relative stability of the collisional drift wave results from a competition between the destabilizing influence of the "time dependent thermal force" and the stabilizing influences of electron dissipation and convective energy loss. In the limit $S \to 0$, the mode is unstable with a growth rate $\gamma \sim \omega_{*T}^2/\nu_e$. As the shear increases, electron collisional dissipation and parallel thermal conduction have a stabilizing effect (scaling as $S^{1/2}$ in Region I and $S^{1/3}$ in Region II) and the growth rate of the mode

decreases. In Region III, the drift mode is always stable with electron dissipative effects completely dominating the destabilizing thermoelectric terms. Finally, in Region IV, the convective energy loss becomes important and the mode is again stable.

Since the eigenfrequencies of the drift mode have been calculated for all values of shear and wavelength (under the restriction $\omega/\nu_{ei} \ll 1$), the stability of a given mode for a given set of parameters can be calculated. It would, however, be useful to obtain a shear stability criterion which guarantees stability for all modes $k_\perp$ for a given shear. To do this, we note that both $b = k_\perp^2 \rho_s^2$ and $S \propto \omega_{*T} \propto k_\perp$ are functions of the perpendicular wavelength. Thus, by increasing $k_\perp$ for a fixed shear and collisionality, we may trace out a curve in the S-b phase space. The two classes of possible curves are shown by the dashed lines A and B in Fig. 1 for $(M/m)^{1/2} L_T \nu_e / L_s^2 \nu_e \gtrless 1$, respectively. For case A, the only possible unstable modes are those in Region II. The conditions $\gamma > 0$ with $S < 1$ and $\omega/\nu_{ei} < 1$ yield the constraint

$$1, \left(\frac{M}{m} \frac{L_T^2}{L_s^2}\right)^{-1} \gtrsim \omega/\nu_{ei} \gtrsim \left(\frac{M}{m} \frac{L_T^2}{L_s^2}\right), \tag{35}$$

which can only be satisfied for $L_s/L_T \gtrsim (M/m)^{1/2}$. Thus, for stability we require

$$L_s/L_T \lesssim (M/m)^{1/2}. \tag{36}$$

This stability threshold is rather sensitive to the value of α' and therefore should only be considered approximate. In Case B, the modes can be unstable in either Region I or Region II. The modes have larger growth

rate in Region I with $b > 1$, so that if the drift wave is stable here it will also be stable in the other regions of Fig. 1. In Region I with $b > 1$, the condition $\gamma > 0$ with $\omega/\nu_e < 1$ and $S < 1$ again yields the constraint on ω/ν_e given in Eq. (35); so all modes will again be stable when the inequality in Eq. (36) is satisfied.

Relevance to Tokamak Discharges

We now turn our attention to the importance of the ∇T_e-modified drift waves to tokamak discharges. Consider modes with $k_\perp \rho_s \simeq 1$; then, the inequality $\omega \simeq \omega_* \simeq k_\perp \rho_s c_s / L_n < \nu_e$ requires $L_c/qR < (M/m)^{1/2}(a/qR)$, which is difficult to satisfy in many tokamak discharges. (L_c is the collisional mean free path.) Thus, drift wave specialists have tended to regard tokamaks as being collisionless or nearly collisionless, and instabilities such as the dissipative trapped electron instability or the collisionless ∇B resonance-driven drift wave are considered to be more important than the collisional drift wave. On the other hand, there are still large numbers of collisional modes present even in the highest temperature discharges. The condition $\omega_* < \nu_e$ for all modes in a tokamak requires the inequality $L_c/qR > (M/m)^{1/2}(a/\rho_s)(a/qR)$, which is far from being satisfied in present machines. There is, at present, no compelling theoretical evidence for believing that collisional drift waves are more important than collisionless modes or *vice versa*.

Density fluctuations have been experimentally measured in a variety of tokamak discharges by a number of different techniques including microwave, CO_2, and far infra-red scattering, and probes. The spectra are characteristically peaked at the longest measurable wavelengths (lowest frequency) while the fluctuations are peaked at a minor radius $r_s \gtrsim a/2$. In Table I,

we summarize the data of some published measurements of density fluctuations in tokamaks. The first five columns list, respectively, the tokamak on which the measurements were made, the position (minor radius) of the fluctuation measurements, the local temperature, the local density, and the local Z_{eff}, as reported by the authors. In instances where only peak (r=0) expressions for T_e and n_e were reported, we approximated $T_e(r_s) \approx T_e(0)/2$ and $n_e(r_s) \approx .75\ n_e(0)$. In the sixth column, we have tabulated the 90^o electron-ion scattering collision frequency, ν_{ei}, as computed from the local plasma parameters. Finally in the last column is the spectral half width, $\omega_{hm} = 2\pi f_{hm}$, of the observed fluctuations, where f_{hm} is the frequency at which $S(\omega)$ falls approximately to half of its peak value. Note that $\omega_{hm} \lesssim \nu_{ei}$ for all the reported measurements. It should, however, be emphasized that the PLT data reported in Ref. 4 was taken before neutral beam heating was undertaken and that this data may therefore not be representative of present PLT operation. Nevertheless, Table I indicates that collisional modes are quite likely to be more important in present-day tokamaks than has been previously believed.

The observation of collisional modes in tokamaks does not guarantee that the fluctuations are destabilized by the mechanism reported in this paper. The shear stabilization condition reported in this paper, [Eq. (36)], is not well satisfied in present tokamak discharges so that instability is probable within the limitations of the present model. However, finite β effects were found to have a stabilizing effect on this mode in previous numerical computations.[12] The effect of finite β on the present fluid description of this instability is not yet determined.

Perhaps the most important conclusion of this work is that the temperature gradient strongly modifies the structure of collisional drift modes.

Collisional modes in present tokamak discharges would fall along curve A in Regions II or III of Fig. 1 so that the modes would be localized and the convective loss of wave energy not important. This conclusion may eliminate the original motivation for studying the effect of toroidal coupling on collisional drift waves, i.e., to nullify the convective loss of wave energy by coupling adjacent poloidal modes. However, the existence of a new unstable branch of the collisional drift wave in a $\nabla T_e \neq 0$ plasma, analogous to the "toroidicity-induced" branch for $\nabla T_e = 0$ plasmas,[20] can not be discounted.

ACKNOWLEDGMENTS

We would like to acknowledge many beneficial conversations with P. N. Guzdar and Y. C. Lee.

This work was supported in part by the Department of Energy, Office of Naval Research, and the Univ. of Md. Center for Theoretical Physics.

REFERENCES

1. E. Mazzucato, Phys. Rev. Lett. 36, 792 (1976).
2. C. M. Surko and R. E. Slusher, Phys. Rev. Lett. 37, 1747 (1976).
3. R. E. Slusher and C. M. Surko, Phys. Rev. Lett. 40, 400 (1978).
4. E. Mazzucato, Phys. Fluids 21, 1063 (1978).
5. S. J. Zweben, C. R. Menyuk and R. J. Taylor, Phys. Rev. Lett. 42, 1270 (1979); S. J. Zweben and R. J. Taylor, to be published.
6. A. Semet, A. Mase, W. A. Peebles, N. C. Luhmann, Jr., and S. J. Zweben, Phys. Rev. Lett. 45, 445 (1980).
7. Equipe TFR, in Plasma Physics and Controlled Nuclear Fusion Research (International Atomic Energy Agency, Vienna, 1980), to be published.
8. A. Gondhalekar, D. Overskei, R. Parker, and J. West, MIT Report PFC/RR-78-15 (1978).
9. L. D. Pearlstein and H. L. Berk, Phys. Rev. Lett. 23, 220 (1969).
10. D. W. Ross and S. M. Mahajan, Phys. Rev. Lett. 40, 324 (1978); K. T. Tsang, P. J. Catto, J. C. Whitson, and J. Smith, Phys. Rev. Lett. 40, 327 (1978); T. M. Antonsen, Phys. Rev. Lett. 41, 33 (1978); P. N. Guzdar, L. Chen, P. K. Kaw, and C. Oberman, Phys. Rev. Lett. 40, 1566 (1978).
11. S. M. Mahajan and D. W. Ross, Phys. Fluids 22, 1506 (1978).
12. C. L. Chang, J. F. Drake, N. T. Gladd, and C. S. Liu, Phys. Fluids 23, XXXX (1980).
13. A. B. Hassam, Phys. Fluids 23, 38 (1980); Phys. Fluids 23, XXXX (1980).
14. J. F. Drake, N. T. Gladd, C. S. Liu, and C. L. Chang, Phys. Rev. Lett. 44, 994 (1980); Phys. Fluids 23, 1182 (1980).

15. L. Chen, P. N. Guzdar, J. Y. Hsu, P. K. Kaw, C. Oberman, and R. White, Nucl. Fusion 19, 373 (1979).

16. S. I. Braginskii, in **Reviews of Plasma Physics**, edited by M. A. Leontovich (Consultants Bureau, New York, 1965), Vol. I, p. 205.

17. J. F. Drake and Y. C. Lee, Phys. Fluids 20, 1341 (1977).

18. R. D. Hazeltine, D. Dobrott, and T. S. Wang, Phys. Fluids 18, 1778 (1975).

19. M. Abramowitz and I. A. Stegun, Handbook of Mathematical Functions, NBS Appl. Math. Series 55 (1964).

20. J. Hastie, K. Hesketh, and J. B. Taylor, Nucl. Fusion 19, 1223 (1979); L. Chen and C. Z. Cheng, (to be published).

FIGURE CAPTIONS

Fig. 1. The four regimes of the VT_e-modified drift wave as shown in the S-b phase space, where $S = (ML_n^2/mL_s^2)(\omega_{*T}/\nu_e)$ and $b = k_L^2\rho_s^2$ represent the magnetic shear strength and perpendicular wavelength, respectively.

Fig. 2. Anti-Stokes (solid) and Stokes (dashed) structure for the VT_e-modified drift wave. The ion sound turning points fall outside the domain of the plot.

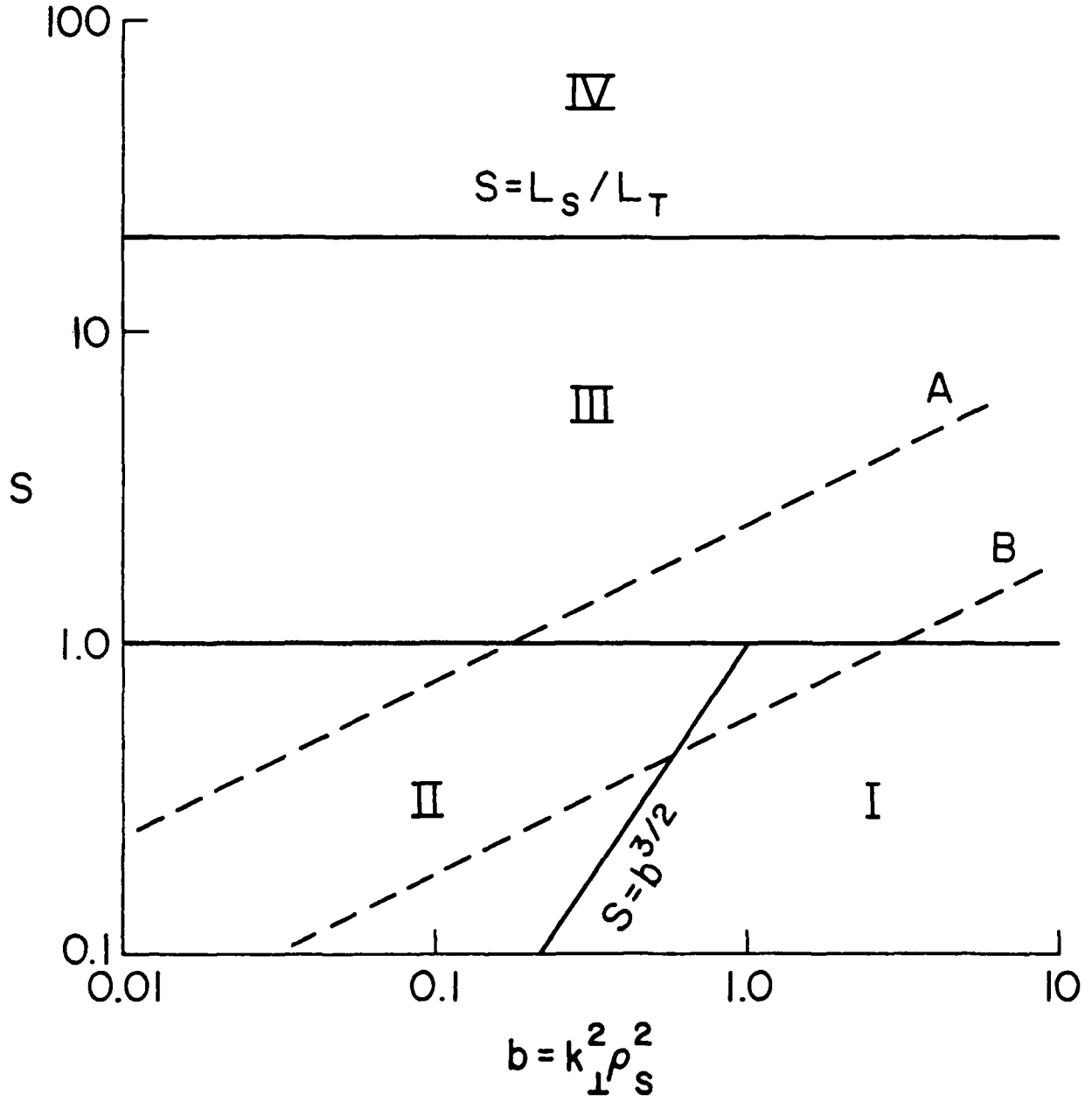
100
10
1.0
0.1
S
IV
S=L_S/L_T
III
A
B
II
I
S=b^{3/2}
0.01
0.1
1.0
10
b=k_⊥^2ρ_s^2

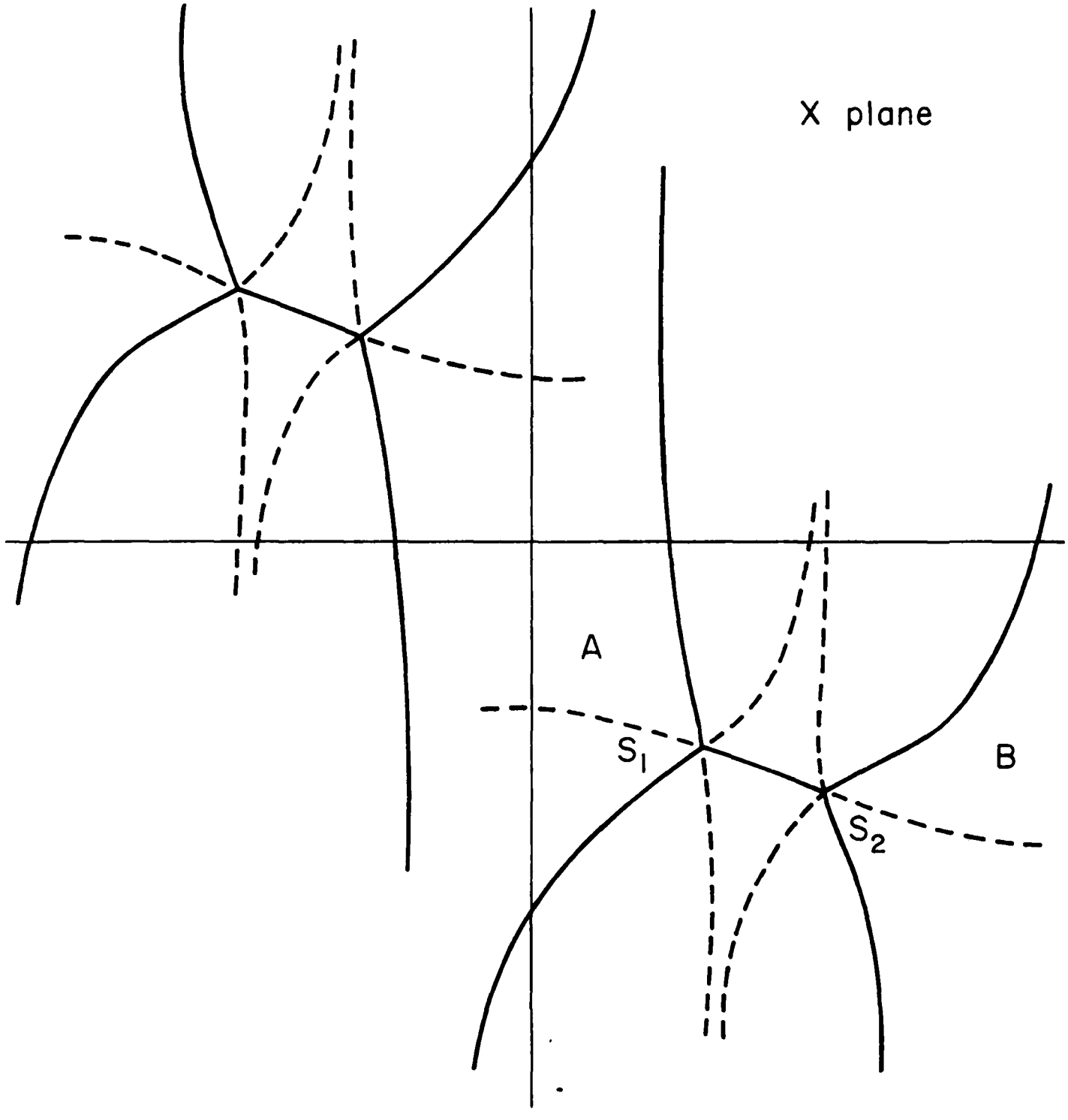
X plane
A
B
S_1
S_2

Table I

Tokamak Fluctuations Data

Tokamak	r_s(cm)	$T_e(r_s)$Kev	$n_e(r_s)(10^{13}/cm^3)$	Z_{eff}	ν_{ei}(MHz)	ω_{hm}(MHz)
ATC[a]	~ 8	.4	1	5	1.0	1.2
Alcator[b]	7	.23	2	1	.8	.9
PLT[c]	~22	.7	3	5	1.8	.6
Macrotor[d]	25	.05	0.3	1	1.3	.3
TFR[e]	10	.5	5	2.5	1.7	1.8
Microtor[f]	5	.27	2.7	1	.9	.3

[a]Ref. 1,2 [b]Ref. 3 [c]Ref. 4

[d]Ref. 5 [e]Ref. 7 [f]Ref. 6